Solar Direct Torque Controlled Induction Motor Drive for Industrial Applications

Aurobinda Panda*‡, M.K. Pathak**, S.P. Srivastava***

*Department of Electrical Engineering, Indian Institute of Technology Roorkee, Uttrakhand, India

(aurobind.panda@gmail.com, mukeshfee@iitr.ac.in, satyafee@iitr.ac.in)

‡ Corresponding Author; Aurobinda Panda, Department of Electrical Engineering, Indian Institute of Technology Roorkee, Roorkee, Uttrakhand, India-247667, aurobind.panda@gmail.com

Received: 20.11.2013 Accepted: 21.11.2013

Abstract- With the continuous decrease of the cost of solar cells, there is an increasing interest in photovoltaic (PV) system applications. Electric motors powered by solar energy are one of the most important applications now-a-days, such as in water pumping systems, electric vehicles etc. This paper investigates a photovoltaic-electro mechanic chain, composed of a PV generator, an impedance adapter DC–DC converter, inverter and a direct torque controlled induction machine. The PV generator is forced to operate at its maximum power point (MPP) by using a fuzzy based maximum power point tracking algorithm. Induction motor performance is obtained at different irradiation and temperature conditions. Simulation results show the effectiveness and feasibility of such an approach.

Keywords- Photovoltaic, Maximum PowerPoint Tracking, Direct torque control, PV generator.

1. Introduction

Given the current concerns of global warming, environmental pollution, energy security and industrial competitiveness, there is increasing pressure on industry to use modern, clean and efficient sources of energy. Now with the scarcity of conventional source of energy, the renewable source of energy like solar, wind and biomass-based technologies have shown considerable potential and are waiting to be tapped not just for domestic use but industrial energy purposes as well. Solar electrical energy generation provides several advantages with respect to other energy sources like it uses the inexhaustible world-wide available sunlight as a source of energy; it does not generate environmental pollutants. This paper focuses on the use of solar energy on induction motor drive which is by far the workhorse in industrial applications.The advancement of power semiconductor devices and the evolvement of several control techniques for converter topologies have made the induction motor drives to become the first choice for many industrial applications [10]. In addition to its advantages, such as speed capability, robustness, cheapness and ease of maintenance, when used with either vector control or direct control scheme, the induction motor can compete with the DC motor in high-performance applications [8].However with some major complexities like coordinate transformation, inclusion of shaft encoder and parameter dependency making the vector controlled drives less popular [4]. To overcome these problems, direct torque control (DTC) technique was introduced. DTC uses an induction motor model to predict the voltage required to achieve a desired output torque. By using only current and voltage measurements it is possible to estimate the instantaneous stator flux and output torque. An induction motor is then used to predict the voltage requirement to drive flux and torque to the demanded values with in a fixed time period. In DTC it is possible to control directly the stator flux and torque by selecting inverter states. In direct torque controlled induction motor drive the dynamic performance of the system is mainly influenced by the PWM method used [1]. PWM methods for the most commonly used voltage source inverters impress either the voltages, or the currents into the stator windings of the machine. Many authors have been proposed different PWM techniques for improving the dynamic performance and also to minimize the torque ripple [1-5].Some have used a space-vector modulation, which subdivides the switching period into three or more states, to synthesize the voltage vectors in order to generate minimum torque ripple [7],[9]. SVM provides better utilization of the dc bus voltage and lower harmonics. The inconsistent nature

of solar energy and the comparatively high cost of PV module throw a big challenge in front of researchers to increase the overall efficiency of the solar system. So in case of solar direct torque controlled induction motor drive it is essential to optimally use the available dc voltage generated from Photovoltaic module. For this reason space vector modulation technique has been used for this proposed solar direct torque controlled induction motor drive. Also a fuzzy based maximum power point tracking controller has been used for extracting maximum power from the PV module.

2. Contribution of the Paper

In this paper, we present a solar direct torque control scheme that can be used for industrial applications. The main features of this paper are as follows.

1) Steady state torque control is achieved even at low irradiation and temperature conditions. Also we are able to maintain a low THD during unfavorable atmospheric conditions.
2) Atmospheric variation plays a big role in power generation from PV module and it affects the performance of induction motor drive. For this a fuzzy based maximum power point tracking controller is used to extract maximum power from the PV module at varying atmospheric conditions.
3) Dynamic response for a step in torque command depends upon the ability of the controller to apply the maximum switching state vector that produces the fastest possible acceleration/deccelaration of the stator flux vector. In order achieve this space vector modulation is used.

3. Proposed Solar Direct Torque Controlled Induction Motor Drive

Fig.1 presents the complete block diagram of the proposed solar direct torque controlled induction motor drive. Here the 3-phase induction motor is fed from a PV module through a DC-DC converter and an Inverter. The dc-dc converter has been used to extract the maximum power from the PV module. In this paper fuzzy logic based MPPT controller has been proposed to reduce the maximum power tracking time. For the direct torque control of induction motor, space vector modulation technique has been used to improve the dynamic performance of the whole system.

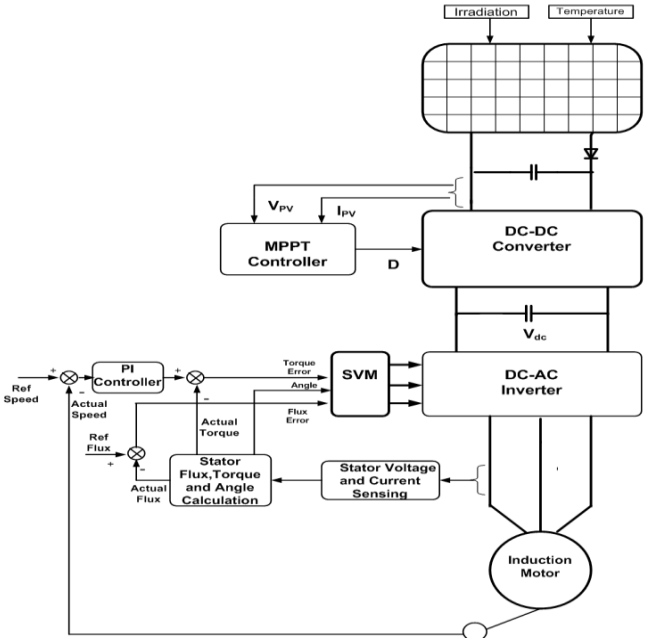

Fig. 1. Block diagram of solar direct controlled Induction motor drive

3.1. Modeling of PV Generator

The solar cell is the basic unit of a photovoltaic module and it is the element in charge of transforming the sun rays or photons directly into electric power. The solar cell used is the PN junction, whose electrical characteristics differ very little from a diode.

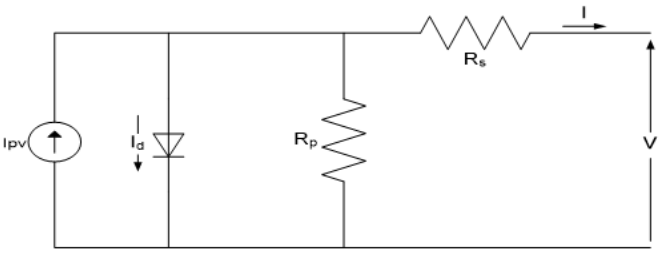

Fig. 2. Equivalent circuit of a PV Cell

The equivalent circuit of a practical PV cell is shown in fig.2.The characteristic equation of a PV cell is the output current produced by it and is expressed as [3]-[4],

$$I = I_{PV} - I_0\left[e^{\left(\frac{V+R_sI}{V_t a}\right)} - 1\right] - \frac{V+R_sI}{R_p} \qquad (1)$$

Where I_{PV}=Current generated by the incident solar radiation

I_0=Reverse saturation or leakage current of the diode

V_t =Thermal voltage of PV module with N_s PV cell connected in series

$= N_sKT/Q$

K=Boltzmann constant=1.3806503 x 10^{-23} J/K

Q=Electron Charge=1.60217646 x 10^{-19} C

T=Temperature in Kelvin

a=Diode ideality constant (1<a<1.5)

PV cells connected in parallel increases the total output current of the PV module whereas cells connected in series increases the total output voltage of the module.

For simulation purpose all information can be found on the manufacturer PV module datasheet like, open circuit voltage, short circuit current, the voltage at the MPP, the current at the MPP, the open circuit voltage/temperature coefficient (K_V), the short circuit current/temperature coefficient (K_I), and the maximum experimental peak output power ($P_{max,\ e}$).These information are always given at standard test condition i.e. at 1000 W/m^2 irradiation and 25^0C temperature. The other information like the light generated current, diode saturation current, diode ideality constant, series and parallel resistance which are not mentioned in manufacturer datasheet but required for the simulation purpose can be evaluated as follows[5].

The current generated by the incident solar radiation is depends linearly on the solar irradiation and is also influenced by the temperature according to the following equation [3], [11].

$$I_{PV} = [I_{PV,n} + K_1 \Delta T] \frac{G}{G_n} \quad (2)$$

Where,

$I_{PV,\ n}$ is the light generated current at the nominal condition i.e. at 25°C and 1000W/m^2

ΔT =Actual temperature-Nominal temperature in Kelvin

G=Irradiation on the device surface

G_n=Irradiation at nominal irradiation

The diode saturation current I_0 and its dependence on the temperature may be expressed as [11],

$$I_0 = I_{0,n} \left(\frac{T_n}{T}\right)^3 exp\left[\frac{qE_g}{aK}\left(\frac{1}{T_n} - \frac{1}{T}\right)\right] \quad (3)$$

Where E_g is the band gap energy of the semiconductor and $I_{o,\ n}$ is the nominal saturation current and is expressed as [3], [11],

$$I_{o,n} = \frac{I_{sc,n}}{exp\left(V_{oc,n} \big/ aV_{t,n}\right) - 1} \quad (4)$$

Where $V_{oc,\ n}$=Nominal open circuit voltage of the PV module

Finally the series and parallel resistance of the PV cell can be calculated by any iteration method. Here Newton-Raphson method has been used for solving the characteristics equation (equation 1) to find R_S and R_P values [5].R_S basically depends on the contact resistance of the metal base, the resistance of the p and n bodies, and the contact resistance of the n layer with the top metal grid. The R_P resistance exists mainly due to the leakage current of the p-n junction [3] .The value of R_P is generally too high where as the value of R_S is very low.

3.2. Fuzzy logic Based MPPT Controller

In the fuzzy logic estimator, there are two input variables, which are error and change in error, one output variable which is duty cycle. Each universe of discourse of the eroor, change in error and duty cycle is divided into five fuzzy sets.Tringular membership function have been used here. All the membership function is shown in Figure 3. There are total 25 rules as listed in Table.I.Each control rule can be described using the input variables E, CE and output variables D.Fuzzy logic control generally consists of three stages: fuzzification, rule base and defuzzification. During fuzzification, numerical input variables are converted into linguistic variable based on a membership function. For this MPPT, the inputs to fuzzy logic controller are taken as a change in power w.r.t change in current E and change in voltage error CE.Once E and CE are calculated and converted to the linguistic variables, the fuzzy logic controller output, which is duty ratio D of the power converter, can be looked up in a rule base table. The linguistic variables assigned to D for the different combinations of E and CE is based on the knowledge of the user. Here the rule base is prepared based on P&O algorithm where the current/voltage is repeatedly perturbed by a fixed amount in a given direction, and the direction is changed only if it detects a drop in power between steps. In the defuzzification stage, the fuzzy logic controller output is converted from a linguistic variable to a numerical variable still using a membership function. MPPT fuzzy logic controllers have been shown to perform well under varying atmospheric conditions. However, their effectiveness depends a lot on the knowledge of the user or control engineer in choosing the right error computation and coming up with the rule base table. The equations for error E and change in error CE are given as follows:

$$E = \frac{P(k) - P(k-1)}{I(k) - I(k-1)}$$

$$CE = V(K) - V(k-1)$$

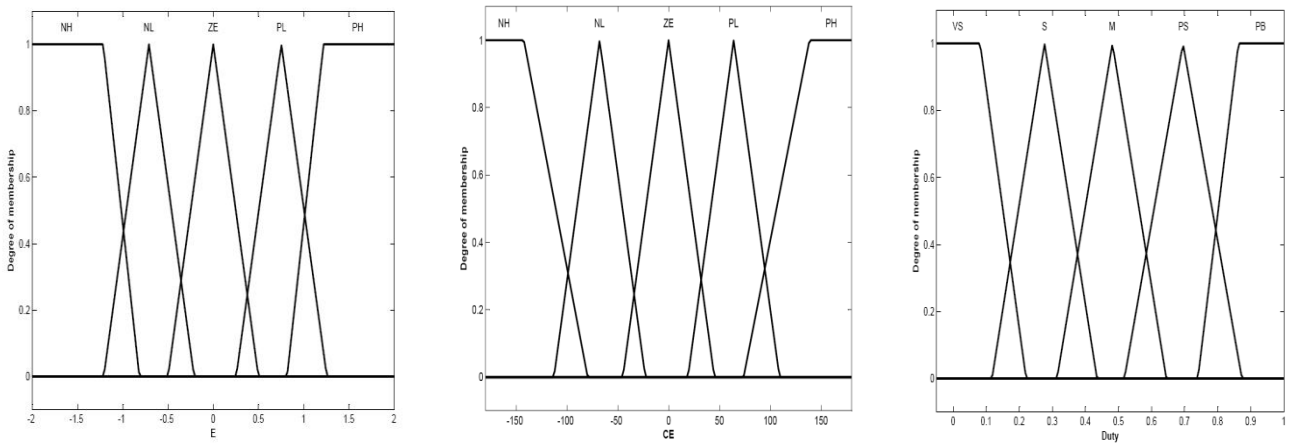

Fig. 3. Membership functions for inputs (E, CE) and output (D) in Fuzzy logic controller based MPPT

Where E and CE are the inputs and D is the output of the fuzzy logic controller.E and CE is having five membership functions each namely, Negative High (NH), Negative Low (NL), Zero (ZE), Positive Low (PL), Positive High (PH).Similarly he output D is also having five membership functions namely, Very Small (VS), small(S), Medium (M), Positive small (PS), Positive Big (PB).

3.3. DTC Induction Motor drive Using SVM

The basic concept of direct torque controlled induction motor drives is to control both stator flux and electromagnetic torque of the machine simultaneously. The direct torque control (DTC) based drives do not require the coordinate transformation between stationary frame and synchronous frame in comparison with the conventional vector controlled drives. The name direct torque control (DTC) is derived by the fact that on the basis of the error between the reference and the estimated values of the torque and flux, it is possible to directly control the inverter states in order to reduce the torque and flux error within limits.

The operating status of the switches in the two-level inverter shown in Fig. 4 can be represented by switching states. The space vector diagram of the two level inverter is presented in fig.5. As indicated in Table II, switching state 'P' denotes that the upper switch in an inverter leg is on and the inverter terminal voltage (VAO, VBO, or VCO) is positive (+Vd) while 'O' indicates that the inverter terminal voltage is (-Vd) due to the conduction of the lower switch. There are eight possible combinations of switching states in the two-level inverter as listed in Table II. The switching state [POO], for example, corresponds to the conduction of S1, S6, and S2 in the inverter legs A, B, and C, respectively. Among the eight switching states, [PPP] and [OOO] are zero states and the others are active states. The operating principle of a DTC drive controlled through the space vector modulation is presented in Fig. 1. Here for the closed loop speed control, the actual speed is first compared with the reference speed. A PI controller is used in speed controller which gives reference torque. This reference torque is compared with actual torque and gives the torque error. Similarly the actual flux is compared with the reference flux and gives the flux error. Finally the flux error, torque error and the angle is fed to a SVM generator, which generates the switching pulses for the inverter. The reference space vector (Vref) for the space vector modulation can be synthesized by three stationary vectors. The dwell time for the stationary vectors essentially represents the duty-cycle time (on-state or off-state time) of the chosen switches during a sampling period Ts of the modulation scheme. The dwell time calculation is based on 'volt-second balancing' principle, that is, the product of the reference voltage Vref and sampling period Ts equals the sum of the voltage multiplied by the time interval of chosen space vectors. Assuming that the sampling period Ts is sufficiently small, the reference vector Vref can be considered constant during Ts. Under this assumption, Vref can be approximated by two adjacent active vectors and one zero vector. For example, when Vref falls into sector I as shown in Fig.6, it can be synthesized by V1, V2, and V0.

Table 1. Rule Base for the proposed FLC

		Change in Error (CE)				
	Duty Cycle ↘	NH	NL	ZE	PL	PH
Error(E)	NH	PS	PB	PB	PS	M
	NL	S	PS	PB	PB	PB
	ZE	PB	M	M	M	S
	PL	VS	S	S	PB	PB
	PH	VS	VS	PB	PB	PB

The volt-second balancing equation is

$$\left.\begin{aligned} V_{ref}T_s &= V_1T_a + V_2T_b + V_0T_0 \\ T_s &= T_a + T_b + T_0 \end{aligned}\right\} \quad (9)$$

Where Ta, Tb, and T0 are the dwell times for the vectors V1, V2 and V0, respectively.

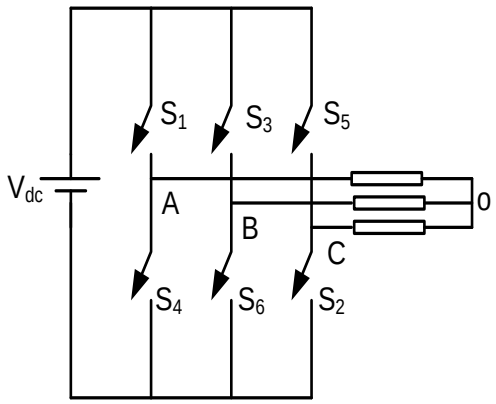

Fig. 4. Two level Inverter

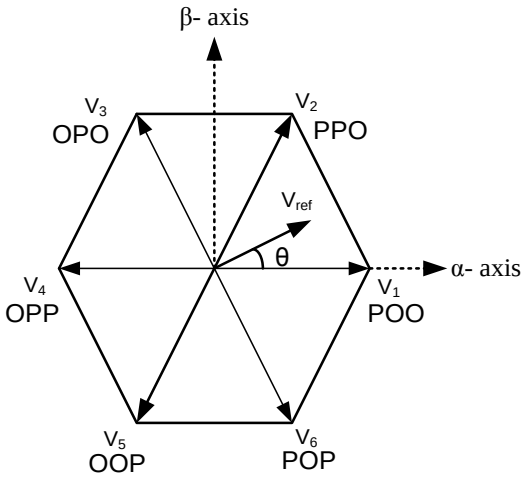

Fig. 5. Space vector diagram for the two-level inverter

Table 2. Switching states in SVM

Space Vector	Switching States	On state Switch	Vector Definition
Zero Vector V_0	OOO	S1, S3,S5	V0 =0
Active Vector V_1	POO	S1, S6,S2	$V_1 = \frac{2}{3}V_d e^{j0}$
V2	PPO	S1, S3,S2	$V_2 = \frac{2}{3}V_d e^{j\pi/3}$
V3	OPO	S4, S3,S2	$V_3 = \frac{2}{3}V_d e^{j2\pi/3}$
V4	OPP	S4, S3,S5	$V_4 = \frac{2}{3}V_d e^{j3\pi/3}$
V5	OOP	S4, S6,S5	$V_5 = \frac{2}{3}V_d e^{j4\pi/3}$
V6	POP	S_1, S_6,S_5	$V_3 = \frac{2}{3}V_d e^{j5\pi/3}$
Zero Vector V7	PPP	S4, S6,S2	V7=0

The space vectors shown in Fig.6 can be expressed as,

$$V_{ref} = V_{ref} e^{j\theta}, V_{1} = \frac{2}{3}V_d, V_{1} = \frac{2}{3}V_d e^{j\pi/3} \text{ and } V_0 = 0 \quad (10)$$

Substituting (10) into (9) and then splitting the resultant equation into the real (α-axis) and imaginary (β-axis) components in the α–β plane, we have

$$\left.\begin{aligned} Re: V_{ref} * cos\theta * T_S &= \frac{2}{3}V_d T_a + \frac{1}{3}V_d T_b \\ Im: V_{ref} * sin\theta * T_S &= \frac{1}{\sqrt{3}}V_d T_b \end{aligned}\right\} \quad (11)$$

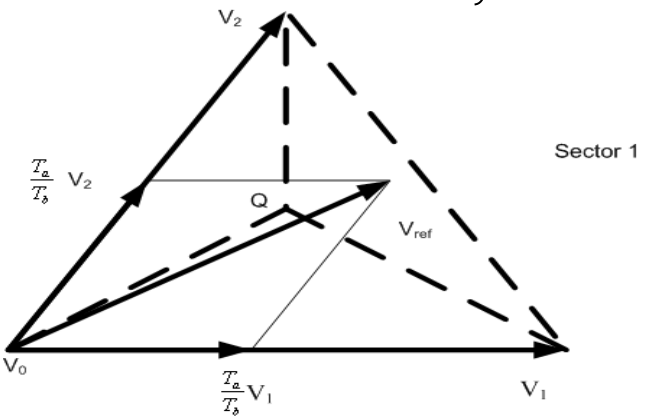

Fig. 6. Synthesize of Voltage Space vector

Solving (11) together with $T_s = T_a + T_b + T_0$, for $0 \le \theta < \pi/3$ yields,

$$\left.\begin{aligned} T_a &= \frac{\sqrt{3}T_S V_{ref}}{V_d} sin\left(\frac{\pi}{3} - \theta\right) \\ T_b &= \frac{\sqrt{3}T_S V_{ref}}{V_d} sin\theta \\ T_0 &= T_S - T_a - T_b \end{aligned}\right\} \quad (12)$$

If V_{ref} lies exactly in the middle between V_1 and V_2 (i.e., $\theta = \pi/6$), the dwell time T_a for V_1 will be equal to T_b for V_2. When V_{ref} is closer to V_2 than V_1, T_b will be greater than T_a. If V_{ref} is coincident with V_2, T_a will be zero.

Although Eq. (12) is derived when V_{ref} is in sector I, it can also be used when V_{ref} is in other sectors provided that a multiple of π/3 is subtracted from the actual angular displacement θ such that the modified angle θ' falls into the range between zero and π/3 for use in the equation, that is,

$$\theta' = \theta - (k-1)\pi/3, \text{For } 0 \le \theta < \pi/3 \quad (13)$$

Where k = 1, 2. . . 6 for sectors I, II . . . VI, respectively.

4. Results and Discussion

The proposed space vector modulation based direct torque induction motor drive fed from a PV module is simulated by using MATLAB simulink software. The parameters of the induction motor and PV module used in simulation are presented in Table III and Table IV

respectively. In order to get a dc link voltage of 450 Volt, 14 PV modules (as mentioned in the datasheet") are connected in series. In Fig.7 and Fig.8 the voltage current characteristics and power-voltage characteristics of the PV module at varying temperature and irradiation condition are presented respectively.

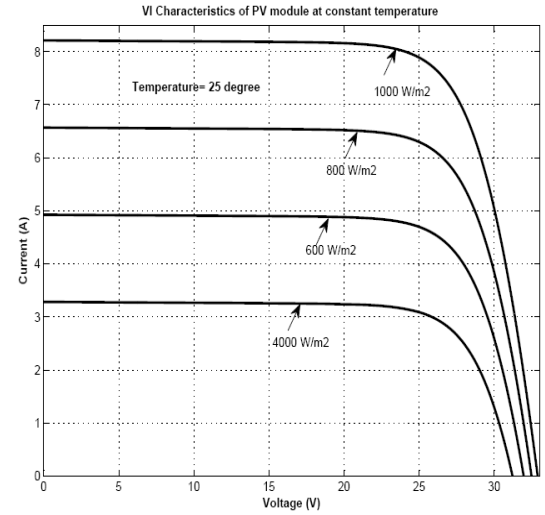

(a)

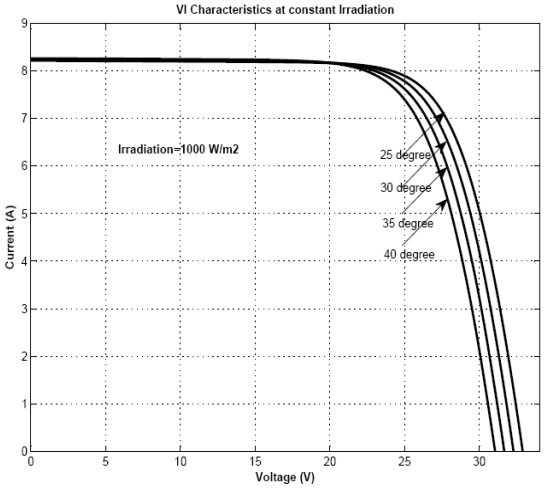

(b)

Fig. 7. VI characteristics of PV module at (a) constant irradiation and varying temperature condition (b)constant temperature and varying Irradiation condition.

The fuzzy logic based maximum power point tracking controller has been used to extract the maximum power of PV module at different atmospheric conditions. In Fig.9 and Fig.10, the maximum power point tacking of PV module at varying irradiation and temperature conditions has been presented. Fuzzy logic controller has been used for this maximum power point tacking of the PV module. From these figures, it can be observed that the maximum power of the PV module has been tracked by the fuzzy controller at 0.2 simulation time. By using this fuzzy based MPPT controller the solar energy can be efficiently used to feed the induction motor drive.

For the direct torque control induction motor drive, the reference speed value is taken as 1400 rpm.At starting induction motor is made to run at no-load condition and at 0.8 simulation time a load of 6 Nm is connected with the Induction motor. The speed and torque response curves of proposed DTC-SVM fed from PV module at varying irradiation and temperature conditions are shown in Fig. 11(i) and 11 (ii)respectively. As it can be observed from the simulation results that up to an irradiation of 400 kw/m2 the PV module maintained the dc link voltage at 400 volt and hence the dtc based induction motor drive operate stably up to this condition. Also from the simulation results it can be observed that temperature variation doesn't affect much in these types of systems. Finally in Fig.12, the torque ripple of the proposed dtc drive has been presented. Here in this case the torque ripple of the induction motor drive is coming as 1Nm which is best suited for industrial applications.

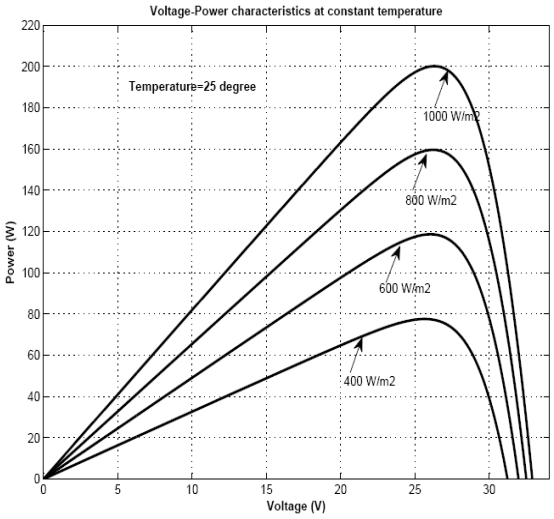

(a)

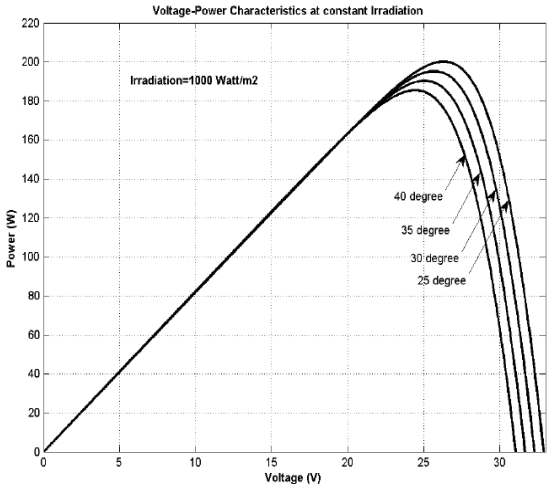

(b)

Fig. 8. Voltage-Power Characteristics of PV module at (a) constant irradiation and varying temperature condition (b)constant temperature and varying Irradiation condition

Table 3. Parameter of Induction motor

Power Rating	4 HP
Stator Voltage	400 Volt
Frequency	50 Hz
Number of Poles	4
Stator Resistance	1.405 ohm
Stator leakage Inductance	0.005839 H
Rotor Resistance	0.451 ohm
Rotor leakage Inductance	0.005839 H
Mutual Inductance	0.1486 H
Inertia	0.0131 kg m2

Table 4. Data sheet of PV Module

Open Circuit Voltage(VOC)	32.9 Volt
Short Circuit Current (ISC)	8.21 Amp
Voltage at MPP(VMPP)	26.5 Volt
Current at MPP (IMPP)	7.6 Amp
Maximum Power	200.143 Watt
Voltage/Temp Coefficient(KV)	-0.1230 Volt/0C
Current/TemperatureCoefficient	0.032 Amp/0C

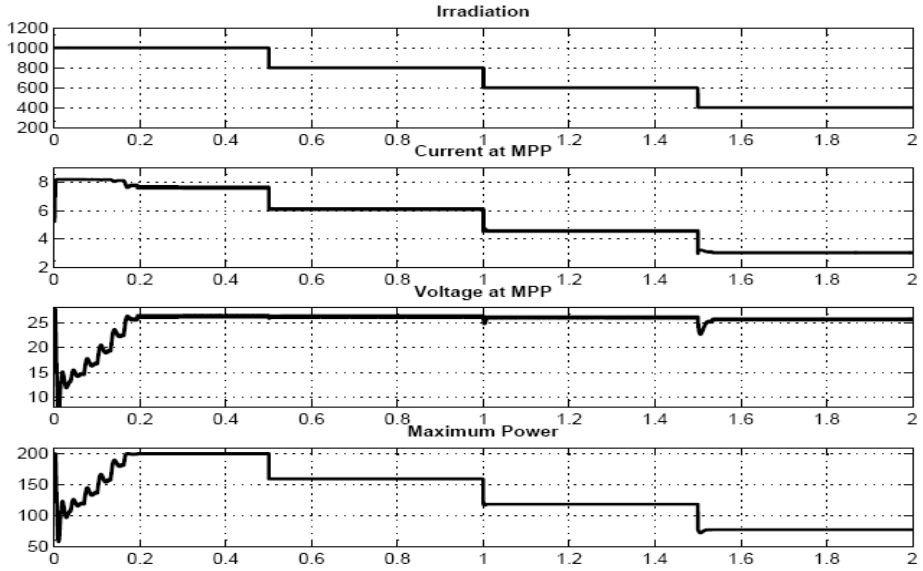

Fig. 9. Maximum power point tracking of PV module by using Fuzzy logic based controller at varying irradiation condition

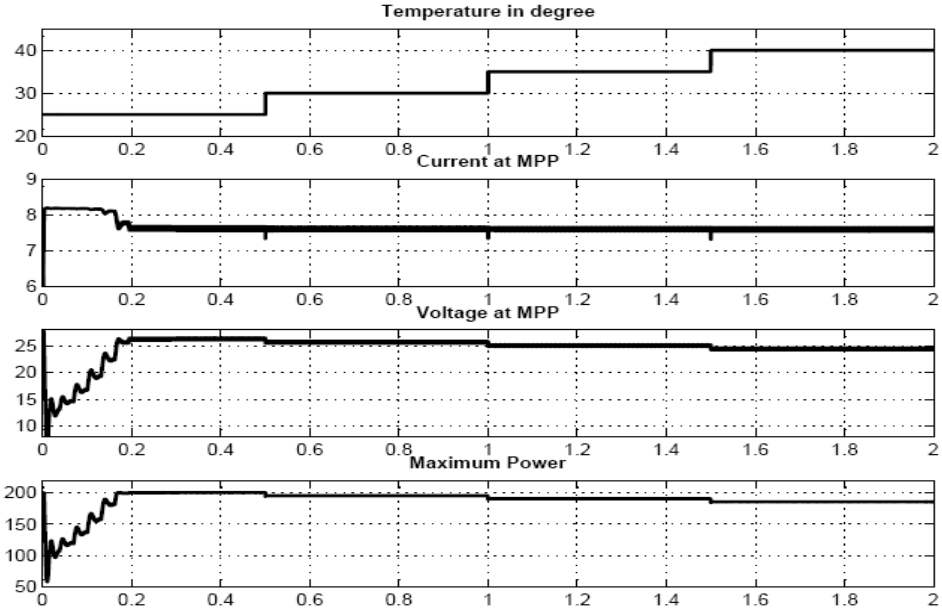

Fig. 10. Maximum power point tracking of PV module by using Fuzzy logic based controller at varying temperature condition

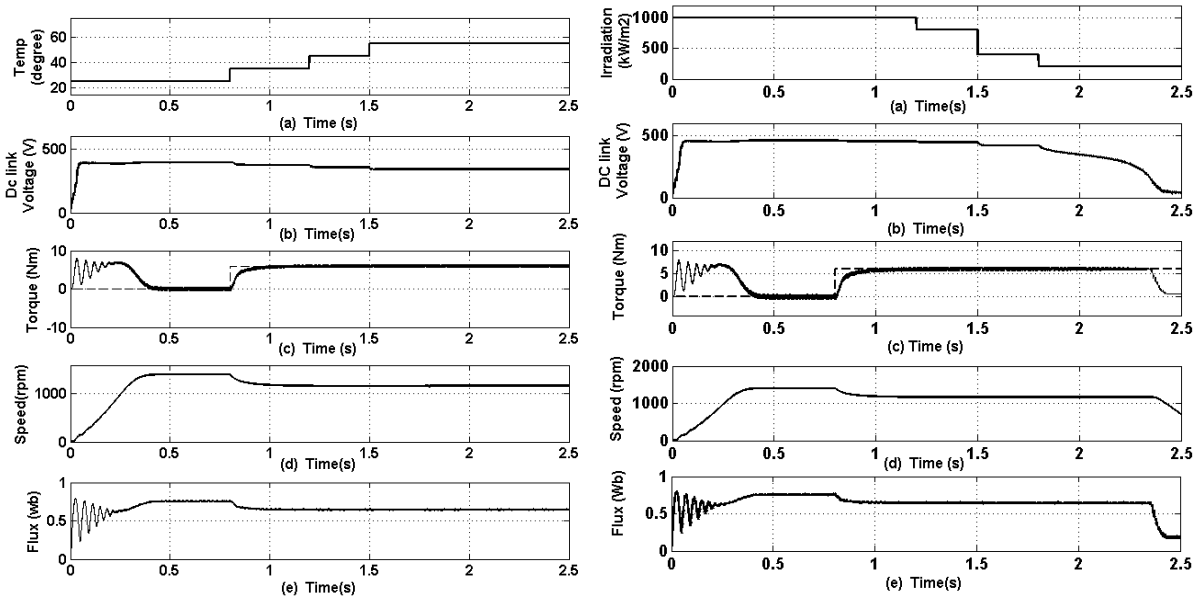

(i) (ii)

Fig. 11. Performance of direct torque controlled induction motor drive (i) at varying irradiation condition (ii) at varying temperature condition

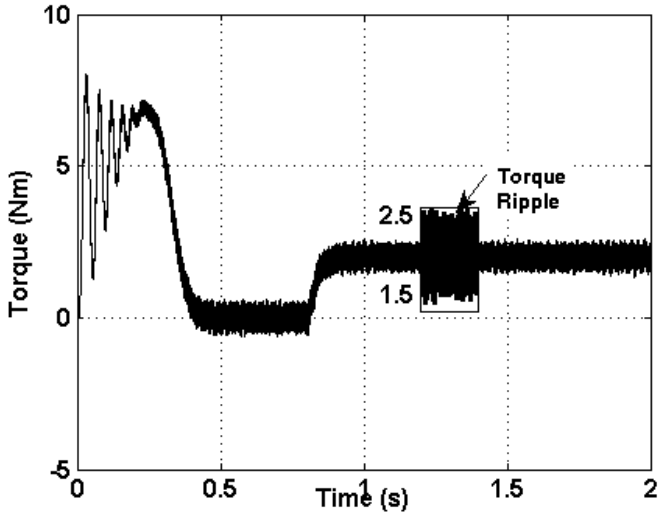

Fig. 12. Torque ripple in DTC based induction motor drive

5. Conclusion

This paper presented a SVM based solar direct torque controlled induction motor drive. By using a fuzzy based maximum power point tracking, solar power is efficiently extracted and fed to a direct torque controlled induction motor drive. Space vector modulation is used for the control part and it improved the dynamic performance of the complete system up to a great extent. Even at load variation the induction motor was able to reach its steady state in a very smooth manner. The controller is set to adapt to changing atmospheric conditions. At different irradiation and temperature condition the induction motor is fed from the PV module .It had been observed that even at low operating condition this proposed system works efficiently with a very low torque ripple in induction motor.

References

[1] J. Holtz, "Pulse width modulation-a survey," IEEE Trans. Ind. Electron.,vol. 38, no. 5, pp. 410-420, Oct. 1992.

[2] G. Juhasz, S. Halasz, and K. Veszpremi, "New aspects of a direct torque controlled induction motor drive," in Proc. IEEE Int. Conf. Industrial Technology, Jan. 2000, pp. 43-49.

[3] D. Casadei, G. Serra, and A. Tani, "Implementation of a direct torque control algorithm for induction motors based on discrete space vector modulation," IEEE Trans. Power Electron., vol. 15, no. 4, pp. 769-777,Jul. 2000.

[4] T. G. Habetler, F. Profumo, M. Pastorelli, and M. Tolbert, "Direct torque control of induction machines using space vector modulation," IEEE Trans. Ind. Application., vol. 28, no. 5, pp. 1045-1053, Sep./Oct. 1992.

[5] J.K. Kang and S.K. Sul, "New direct torque control of induction motor for minimum torque ripple and constant switching frequency," IEEE Trans. Ind. Application., vol. 35, pp. 1076-1082, Sep./Oct. 1999.

[6] El Moucary, C.; Mendes, E.; Razek, A.; , "Decoupled direct control for PWM inverter-fed induction motor drives," IEEE Transactions on Industry Applications, vol.38, no.5, pp. 1307- 1315,Sep/Oct,2002.

[7] Idris, N.R.N.; Yatim, A.H.M.;, "Direct torque control of induction machines with constant switching frequency and reduced torque ripple," IEEE Transactions on Industrial Electronics , vol.51,no.4,pp.758-767,Aug.2004.

[8] Casadei, D.; Profumo, F.; Serra, G.; Tani, A.; "FOC and DTC: two viable schemes for induction motors torque

control," IEEE Transactions on Power Electronics , vol.17, no.5, pp. 779- 787, Sep 2002

[9] Attaianese, C.; Perfetto, A.; Tomasso, G.; , "A space vector modulation algorithm for torque control of inverter fed induction motor drive," IEEE Transactions on Energy Conversion, vol.17, no.2, pp.222-228, Jun 2002

[10] Chattopadhyay, A.K., "Alternating Current Drives in the Steel Industry," IEEE Industrial Electronics Magazine, vol.4, no.4, pp.30-42, Dec. 2010